

# TeV neutrinos from core collapse supernovae and hypernovae

Soebur Razzaque,<sup>1</sup> Peter Mészáros<sup>1,2,3</sup> and Eli Waxman<sup>4</sup>

<sup>1</sup>*Department of Astronomy & Astrophysics, Department of Physics,  
Pennsylvania State University, University Park, PA 16802, USA*

<sup>2</sup>*Institute for Advanced Study, Princeton, NJ 08540, USA*

<sup>3</sup>*Department of Atomic Physics, Eötvös University,  
Hungarian Academy of Sciences, Budapest, Hungary*

<sup>4</sup>*Physics Faculty, Weizmann Institute of Science, Rehovot 76100, Israel*

(Dated: July 24, 2018)

A fraction of core collapse supernovae of type Ib/c are associated with Gamma-ray bursts, which are thought to produce highly relativistic jets. Recently, it has been hypothesized that a larger fraction of core collapse supernovae produce slower jets, which may contribute to the disruption and ejection of the supernova envelope, and explain the unusually energetic hypernovae. We explore the TeV neutrino signatures expected from such slower jets, and calculate the expected detection rates with upcoming Gigaton Cherenkov experiments. We conclude that individual jetted SNe may be detectable from nearby galaxies.

PACS numbers: 97.60.Bw, 96.40.Tv, 98.70.Sa

Core collapse supernovae (SNe) are known sources of 1-10 MeV neutrinos, as detected from SN 1987A [1]. Previously, 100 TeV neutrinos were predicted from protons accelerated in internal shocks in relativistic jets associated with gamma-ray burst (GRB) event [2], independently of any SN connection. Long duration ( $\gtrsim$  several seconds) GRBs are now known, in several cases, to be associated with SN type Ib/c events triggered by a stellar core collapse which is contemporaneous with the GRB event [3]. The relativistic jets from such core collapses are expected to produce a  $\sim$  TeV neutrino precursor burst, while the jet is making its way out of the collapsing stellar progenitor [4], and this may be present even if the jet does not manage to burrow through the stellar envelope, i.e. choked bursts which are  $\nu$  bright, but  $\gamma$  dark. These previous TeV neutrino predictions assumed jets, with bulk Lorentz factors  $\Gamma_b \gtrsim 100$ . The frequency of highly relativistic jets in SN like events is at most comparable to the ratio of GRB to the average core-collapse SN events,  $\lesssim 10^{-3}$ .

The deposition of bulk kinetic energy from a jet into the stellar envelope may be a powerful contributor to the triggering of a core collapse SN or SN Ib/c [5] and/or to the disruption of the envelope [6]. Only a small fraction of core-collapse SNe appear to be associated with GRBs [7]. However, a significantly larger fraction of SNe may be endowed with slower jets, of  $\Gamma_b \sim \text{few}$  [6, 8, 9, 10], which may also give rise to “orphan” radio afterglows not associated with detected  $\gamma$ -ray emission [11]. In this Letter, we point out that SNe endowed with slow jets will be detectable sources of multi-GeV to TeV neutrinos. Since the occurrence rate per galaxy of SNe is much larger than for GRBs, the chances of one occurring nearby is significantly enhanced. Hyperenergetic SNe (hypernovae) will be fewer in number ( $\sim 10\%$  of type Ib/c rate [12]), but will have a higher neutrino flux. We calculate the neutrino fluence from such slow-jet SNe within the nearest 20

Mpc, and the corresponding neutrino detectability with upcoming kilometer scale Cherenkov detectors in Antarctica and in the Mediterranean [13].

*Jet dynamics.*— We take a jet, with  $\Gamma_b = 10^{0.5}\Gamma_{b,0.5}$ , inside the SN progenitor star. The corresponding jet opening angle is  $\theta_j \sim 1/\Gamma_b$ . With a variability time  $t_v = 0.1t_{v,-1}$  s at the jet’s base, internal shocks occur in the jet at a collision radius  $r_j = 2\Gamma_b^2 ct_v \approx 10^{10.8}\Gamma_{b,0.5}^2 t_{v,-1}$  cm, which is inside the progenitor star (typically a Wolf-Rayet star of  $\sim 10^{11}$  cm radius for a SN Ib, or larger for other type II SN). Typical jet energy, inferred from GRBs, is  $E_j \sim 10^{51.5}E_{51.5}$  ergs while inside the progenitor star. By analogy with the GRB case, we assume that a fraction  $\varepsilon_e \sim 0.1\varepsilon_{e,-1}$  of  $E_j$  is converted into relativistic electron kinetic energy in the internal shocks, which then synchrotron radiate in the presence of magnetic fields representing a fraction  $\varepsilon_b \sim 0.1\varepsilon_{b,-1}$  of  $E_j$ .

The volume number density of leptons and baryons present in the jet is  $n'_e = n'_p = E_j/(2\pi r_j^2 m_p c^3 t_j) \approx 10^{20.5}E_{51.5}\Gamma_{b,0.5}^{-4}t_{j,1}^{-1}t_{v,-1}^{-2}$  cm $^{-3}$  in the comoving frame of the jet. Here  $t_j \approx 10t_{j,1}$  s is the typical jet duration. Electrons and protons are expected to be accelerated to high energy in the internal shocks. Typically all electrons cool down by synchrotron radiation within the dynamic time scale  $t'_{\text{dyn}} = t_v/\Gamma_b$ . However, due to the large Thomson optical depth ( $\tau_{\text{Th}} \sim 10^{6.6}E_{51.5}\Gamma_{b,0.5}^{-3}t_{j,1}^{-1}t_{v,-1}^{-1}$ ), synchrotron photons in the jet thermalize to a black body temperature of  $E'_\gamma = [15(\hbar c)^3 E_j \varepsilon_e / (2\pi^4 r_j^2 ct_j)]^{1/4} \approx 4.3E_{51.5}^{1/4}\varepsilon_{e,-1}^{1/4}\Gamma_{b,0.5}^{-1}t_{j,1}^{-1/4}t_{v,-1}^{-1/2}$  keV. Also photons from the shocked stellar plasma do not diffuse into the jet as a result of the high  $\tau_{\text{Th}}$ . The volume number density of thermalized photons produced by the shocks is  $n'_\gamma = E_j \varepsilon_e / (2\pi r_j^2 c E'_\gamma t_j) \approx 10^{24.8}E_{51.5}^{3/4}\varepsilon_{e,-1}^{3/4}\Gamma_{b,0.5}^{-3}t_{j,1}^{-3/4}t_{v,-1}^{-3/2}$  cm $^{-3}$ .

The magnetic field strength in the jet is given by  $B' = [4E_j \varepsilon_b / (r_{\text{jet}}^2 ct_j)]^{1/2} \approx 10^{8.5}E_{51.5}^{1/2}\varepsilon_{b,-1}^{1/2}\Gamma_{b,0.5}^{-2}t_{j,1}^{-1/2}t_{v,-1}^{-1}$  G

in the comoving frame. The corresponding shock acceleration time for protons is  $t'_{\text{acc}} = AE'_p/eB' \approx 10^{-12}(E'_p/\text{GeV})A_1E_{51.5}^{-1/2}\varepsilon_{b,-1}^{-1/2}\Gamma_{b,0.5}^2t_{j,1}^{1/2}t_{v,-1}$  s. The maximum proton energy is limited by requiring this time not to exceed  $t'_{\text{dyn}}$  or other possible proton cooling process time scales.

*Proton cooling time scales.*— The Bethe-Heitler (BH) interaction  $p\gamma \rightarrow pe^\pm$  has a logarithmically rising cross section  $\sigma_{\text{BH}} = \alpha r_e^2 \{(28/9)\ln[2E'_pE'_\gamma/(m_pm_e c^4)] - 106/9\}$ . The  $e^\pm$  pairs are produced at rest in the center of mass (c.m.) frame of the  $p\gamma$  collision. The energy lost by the proton in each interaction is given by  $\Delta E'_p = 2m_e c^2 \gamma'_{\text{c.m.}}$ , where  $\gamma'_{\text{c.m.}} = (E'_p + E'_\gamma)/(m_p^2 c^4 + 2E'_p E'_\gamma)^{1/2}$  is the Lorentz boost factor of the c.m. in the comoving frame. The energy loss rate of the proton is given by  $dE'_p/dt'_{\text{BH}} = n'_\gamma \sigma_{\text{BH}} \Delta E'_p$ . The corresponding proton cooling time is  $t'_{\text{BH}} = E'_p/(dE'_p/dt') = E'_p/(2n'_\gamma \sigma_{\text{BH}} m_e c^2 \gamma'_{\text{c.m.}})$  in the comoving frame.

Protons, in the presence of the same magnetic field which is responsible for the electron synchrotron losses, also suffer synchrotron losses, but over a longer time scale given by  $t'_{\text{syn}} = 6\pi m_p^4 c^3/(\sigma_{\text{Th}} \beta^2 m_e^2 E'_p B'^2) \approx 3.8(E'_p/\text{GeV})^{-1}E_{51.5}^{-1}\varepsilon_{b,-1}^{-1}\Gamma_{b,0.5}^4 t_{j,1}^2 t_{v,-1}^2$  s.

Protons can also transfer energy to photons by inverse Compton (IC) scattering, because of the significantly high photon density ( $n'_\gamma$ ) in the shocks. The IC cooling time in the Thomson limit is given by  $t'_{\text{IC,Th}} = 3m_p^4 c^3/(4\sigma_{\text{Th}} m_e^2 E'_p E'_\gamma n'_\gamma) \approx 3.8(E'_p/\text{GeV})^{-1}E_{51.5}^{-1}\varepsilon_{b,-1}^{-1}\Gamma_{b,0.5}^4 t_{j,1}^2 t_{v,-1}^2$  s. In the Klein-Nishina (KN) limit, the IC cooling time is given by  $t'_{\text{IC,KN}} = 3E'_p E'_\gamma/(4\sigma_{\text{Th}} m_e^2 c^5 n'_\gamma) \approx 10^{-10.5}(E'_p/\text{GeV})E_{51.5}^{-1/2}\varepsilon_{e,-1}^{-1/2}\Gamma_{b,0.5}^2 t_{j,1}^{1/2}t_{v,-1}$  s. The Thomson and the KN limits apply for  $E'_p$  much less or greater than  $m_p^2 c^4/E'_\gamma \approx 10^{5.3}E_{51.5}^{-1/4}\varepsilon_{e,-1}^{-1/4}\Gamma_{b,0.5}^{1/4}t_{j,1}^{1/2}t_{v,-1}$  GeV, respectively, in the comoving frame.

We have plotted the proton acceleration time and the different cooling times in the comoving frame as functions of the proton energy in Fig. 1. Note that the BH cooling time (long dashed line) and the synchrotron cooling time (short dashed line) are first longer and then shorter than the maximum proton acceleration time (thick solid line). The corresponding maximum proton energy can be roughly estimated, by equating the  $t'_{\text{syn}}$  to  $t'_{\text{acc}}$ , as  $E'_{p,\text{max}} \approx 10^{6.3}A_1^{-1}E_{51.5}^{-1/4}\varepsilon_{b,-1}^{-1/4}\Gamma_{b,0.5}^{1/4}t_{j,1}^{1/2}t_{v,-1}$  GeV.

*Pion and muon production and cooling.*— High-energy protons interact with thermal photons in the shocks to produce neutrinos dominantly through  $p\gamma \rightarrow \Delta \rightarrow n\pi^+ \rightarrow \mu^+\nu_\mu \rightarrow e^+ \nu_e \bar{\nu}_\mu \nu_\mu$  channel. The threshold proton energy at  $\Delta$  is  $E'_{p,\text{th}} = 0.3/E'_\gamma \approx 10^{4.8}E_{51.5}^{-1/4}\varepsilon_{e,-1}^{-1/4}\Gamma_{b,0.5}^{1/4}t_{j,1}^{1/2}t_{v,-1}$  GeV and the corresponding optical depth is  $\tau_{p\gamma} \approx 10^{7.8}E_{51.5}^{3/4}\varepsilon_{e,-1}^{3/4}\Gamma_{b,0.5}^{-2}t_{j,1}^{-3/4}t_{v,-1}^{-1/2}$ , both evaluated in the comoving frame. However, low energy protons may also produce  $\Delta$  by interacting with photons from high-energy tail of the black body photon

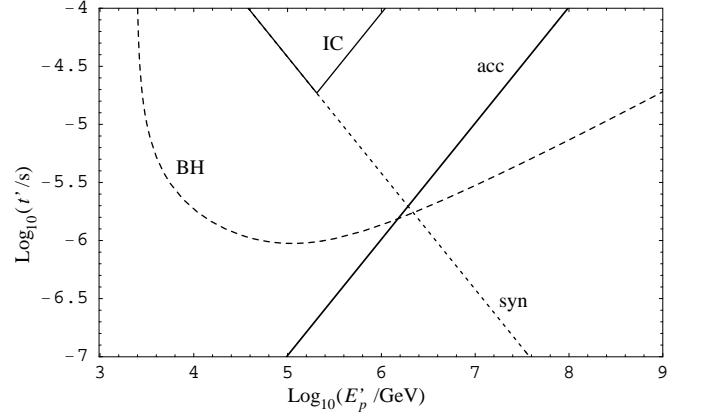


FIG. 1: Proton cooling time scales for different processes, in the comoving frame, as functions of energy. Also shown is the proton shock acceleration time. Burst parameters used are  $E_{\text{sn}} = 10^{51.5}$  erg,  $t_j = 10$  s,  $t_v = 10^{-1}$  s,  $\Gamma_b = 3$ ,  $\varepsilon_e = \varepsilon_b = 0.1$ .

distribution until  $\tau_{p\gamma}$  falls below unity or below the optical depth for other processes such as proton-proton ( $pp$ ) interaction. Similarly, protons with energy above  $E'_{p,\text{th}}$  interact with low energy photons to produce  $\Delta$ .  $pp$  interactions are effective at lower energy compared to  $p\gamma$  interactions. The total pion multiplicity from  $pp$  interactions is of the order unity in the energy range we are considering here [14]. For simplicity, we assume that each  $pp$  interaction produces single pion, the same as  $p\gamma$  interactions, down to the proton energy for which the corresponding neutrino energy is above detection threshold ( $E_{\nu,\text{th}}$ ) on Earth. The available maximum proton energy to produce  $\Delta$ , through  $p\gamma$  interactions, is  $E'_{p,\text{max}} \approx 10^{6.3}$  GeV.

High-energy pions and muons produced in  $p\gamma$  interactions do not all decay to neutrinos, as synchrotron radiation and IC scattering reduce the energy. The synchrotron break energies (below which pions and muons decay before undergoing significant cooling) are found by equating their synchrotron cooling times ( $t'_{\pi,\mu;\text{syn}}$ ) to their decay times ( $\gamma'_{\pi,\mu} t_{\text{dec}}$ ) in the comoving frame, which are  $E'_{\pi,\text{sb}} = 10^2 E_{51.5}^{-1/2}\varepsilon_{b,-1}^{-1/2}\Gamma_{b,0.5}^2 t_{j,1}^{1/2}t_{v,-1}$  GeV and  $E'_{\mu,\text{sb}} = 10^{0.7} E_{51.5}^{-1/2}\varepsilon_{b,-1}^{-1/2}\Gamma_{b,0.5}^2 t_{j,1}^{1/2}t_{v,-1}$  GeV, respectively. The IC cooling time ( $t'_{\text{IC}}$ ) is comparable to the synchrotron cooling time and the two can be combined into a single loss rate  $t'_{\text{cool}} \sim t'_{\text{syn}} + t'_{\text{IC}}$ . For IC losses in the Thomson limit  $t'_{\text{syn}} \approx t'_{\text{IC}}$  while in the KN limit  $t'_{\text{syn}} \ll t'_{\text{IC}}$ , and the neutrino fluence in the presence of these energy losses is suppressed, compared to the fluence obtained assuming pions and muons decay without any energy loss, by a factor

$$\begin{aligned} \zeta(E_{\pi,\mu}) &= t'_{\pi,\mu;\text{cool}}/t'_{\pi,\mu;\text{decay}} \approx t'_{\pi,\mu;\text{cool}}/t'_{\pi,\mu;\text{syn}} \\ &= (E_{\pi,\mu}/E_{\pi,\mu;\text{sb}})^{-2}; \quad E_{\pi,\mu} > E_{\pi,\mu;\text{sb}}. \end{aligned} \quad (1)$$

Thus muons and their decay neutrinos are severely sup-

pressed due to their high energy electromagnetic losses. We calculate the neutrino fluence from pion decay next.

*Neutrino flux.*— The observed isotropic equivalent proton fluence from the SN jet, denoting the quantities in the observer's frame with subscript “ob”, at a luminosity distance  $D_L$ , is  $\mathcal{F}_{p,\text{ob}} = E_j \Gamma_b^2 (1+z)/(2\pi D_L^2 E_{p,\text{ob}}^2 \ln[E_{p,\text{max}}/E_{p,\text{min}}])$ . Here we have assumed a shock accelerated proton energy distribution  $\propto E_p^{-2}$ . The energy and time in the observers frame and in the local rest frame (at red shift  $z$ ) are related by  $E_p = E_{p,\text{ob}}(1+z)$  and  $t_j = t_{j,\text{ob}}/(1+z)$ . The corresponding  $\nu_\mu$  fluence from proton interactions is

$$\mathcal{F}_{\nu,\text{ob}} = \frac{1}{8} \frac{E_j \Gamma_b^2 (1+z)^3}{2\pi D_L^2 E_{\nu}^2 \ln[E_{\nu,\text{max}}/E_{\nu,\text{min}}]} \times \left( \frac{E_\nu}{E_{\nu,\text{sb}}} \right)^{-2} \Theta(E_{\nu,\text{min}} \leq E_\nu \leq E_{\nu,\text{max}}), \quad (2)$$

per SN burst, assuming all shock accelerated protons convert to pions. The factor of 1/8 is due to the fact that in the absence of energy losses, the neutrinos produced by pion decay carry 1/8 of the energy lost by protons to pion production (since charged pions and neutral pions are produced with roughly equal probability, and since the muon neutrino produced in a pion decay carries roughly 1/4 of the pion energy). The neutrino energy range is then  $E_{\nu,\text{ob,min}} - E_{\nu,\text{ob,max}} = E_{\nu,\text{th}} - 0.05\Gamma_b E'_{p,\text{max}}/(1+z) \approx 10^{2.5} - 10^{5.5}/(1+z)$  GeV in the observer's frame on Earth. Here we have assumed  $E_{\nu,\text{th}} = 10^{2.5} E_{\nu,2.5}$  GeV for a typical ice Cherenkov detector such as IceCube. For a SN at  $\sim 20$  Mpc ( $D_L \approx 10^{25.8}$  cm,  $z \sim 0$ ), e.g. in the Virgo cluster, the neutrino fluence would be

$$\mathcal{F}_{\nu,\text{ob}}^* \approx 10^{-3} \left( \frac{E_{\nu,\text{ob}}}{100\text{GeV}} \right)^{-4} \frac{E_{51.5}^{3/2} \varepsilon_{b,-1}^{1/2}}{\Gamma_{b,0.5} D_{25.8}^2 t_{j,1}^{1/2} t_{v,-1}} \text{GeV}^{-1} \text{cm}^{-2}; 10^{2.5} \lesssim E_{\nu,\text{ob}}/\text{GeV} \lesssim 10^{5.5}. \quad (3)$$

To calculate the diffuse neutrino flux, we sum over fluences from all slow-jet SNe distributed over cosmological distances in Hubble time. The SNe rate follows closely the star formation rate (SFR) which can be modeled as  $\dot{\rho}_*(z) = 0.32 h_{70} \exp(3.4z)/[\exp(3.8z) + 45] \text{M}_\odot \text{yr}^{-1} \text{Mpc}^{-3}$  per unit comoving volume [15]. Here  $H_0 = 70 h_{70} \text{km s}^{-1} \text{Mpc}^{-1}$  is the Hubble constant. For a Friedmann-Robertson-Walker universe, the comoving volume element is  $dV/dz = 4\pi D_L^2 c/(1+z)|dt/dz|$  and the relation between  $z$  and the cosmic time  $t$  is  $(dt/dz)^{-1} = -H_0(1+z)\sqrt{(1+\Omega_m z)(1+z)^2 - \Omega_\Lambda(2z+z^2)}$ . Here we have used the standard  $\Lambda$ CDM cosmology with  $\Omega_m = 0.3$  and  $\Omega_\Lambda = 0.7$ .

The number of SNe per unit star forming mass ( $f_{\text{sn}}$ ) depends on the initial mass function and the SN threshold for stellar mass ( $M \sim 8 \text{M}_\odot$ ). A Salpeter model  $\phi(M) \propto M^{-\alpha}$  with different power-law indices can generate different values for  $f_{\text{sn}}$ , e.g.  $\approx 0.0122 \text{M}_\odot^{-1}$  for  $\alpha = 2.35$  [15]

and  $\approx 8 \times 10^{-3} \text{M}_\odot^{-1}$  for  $\alpha = 1.35$  [16]. We adopt the model in Ref. [15] which corresponds to the local type II SNe rate  $\dot{n}_{\text{sn}}(z=0) = f_{\text{sn}} \dot{\rho}_*(z=0) \approx 1.2 \times 10^{-4} h_{70}^3 \text{yr}^{-1} \text{Mpc}^{-3}$  agreeing with data [17].

The distribution of SNe per unit cosmic time  $t$  and solid angle  $\Omega$  covered on the sky can be written as

$$\frac{d^2 N_{\text{sn}}}{dt d\Omega} = \frac{\dot{n}_{\text{sn}}(z)}{4\pi} \frac{dV}{dz} = \frac{\dot{n}_{\text{sn}}(z) D_L^2 c}{(1+z)^2} \left| \frac{dt}{dz} \right|. \quad (4)$$

We assume a fraction  $\xi_{\text{sn}} \lesssim 1$  of all SNe involve jets and a fraction  $1/2 \Gamma_b^2$  of all such jets are pointing towards us. The observed diffuse SNe neutrino flux, using Eq. (2), is then

$$\begin{aligned} \Phi_{\nu,\text{ob}}^{\text{diff}} &= \frac{\xi_{\text{sn}}}{2\Gamma_b^2} \int_0^\infty dz \frac{d^2 N_{\text{sn}}}{dt d\Omega} \mathcal{F}_{\nu,\text{ob}}(E_{\nu,\text{ob}}) \\ &= \xi_{\text{sn}} \frac{c}{32\pi} \frac{E_j}{E_{\nu,\text{ob}}^2} \int_0^\infty dz \frac{\dot{n}_{\text{sn}}(z)/(1+z)}{\ln[E_{\nu,\text{ob,max}}/E_{\nu,\text{th}}]} \\ &\quad \times \left| \frac{dt}{dz} \right| \left( \frac{E_{\nu,\text{ob}}[1+z]}{E_{\nu,\text{sb}}} \right)^{-2} \\ &\quad \times \Theta(E_{\nu,\text{th}} \leq E_{\nu,\text{ob}} \leq E_{\nu,\text{ob,max}}). \end{aligned} \quad (5)$$

We have plotted the diffuse  $\nu_\mu$  flux from all cosmological slow-jet SNe in Fig. 2 by numerically integrating Eq. (5), assuming the maximal fraction  $\xi_{\text{sn}} = 1$ . Also shown are the cosmic ray bounds (WB limits) on the diffuse neutrino flux [2], and the atmospheric  $\nu_\mu$ ,  $\bar{\nu}_\mu$  flux from pion and kaon decays (conventional flux, [18]), compatible with AMANDA data [19].

$$\Phi_{\nu,\text{ob}}^{\text{atm}} = \begin{cases} \frac{0.012 E_{\nu,\text{ob}}^{-2.74}}{1+0.002 E_{\nu,\text{ob}}} ; E_{\nu,\text{ob}} < 10^{5.8} \text{ GeV} \\ \frac{3.8 E_{\nu,\text{ob}}^{-3.17}}{1+0.002 E_{\nu,\text{ob}}} ; E_{\nu,\text{ob}} > 10^{5.8} \text{ GeV}. \end{cases} \quad (6)$$

Figure 2 demonstrates that the diffuse flux is unlikely to be detectable by km-scale telescopes. However, individual nearby SNe may be detectable, as we show below.

*Neutrino event rate.*— The effective area ( $A_{\text{eff}}$ ) of a Cherenkov detector depends on the zenith angle and the energy of the muon that is created by a charged current neutrino-nucleon ( $\nu N$ ) interaction in the vicinity of the detector. IceCube can trigger on muons of energy (which is  $\sim 80\%$  of the neutrino energy) above a few hundred GeV created within  $A_{\text{eff}} \sim \text{km}^2$  [13]. We assumed  $E_{\nu,\text{th}} \sim 300$  GeV, as discussed before. The angular sensitivity of the IceCube detector is  $1^\circ$  for muon tracks with  $< 140^\circ$  zenith angles below 1 TeV. The pointing resolution gets better at higher energy.

The likeliest prospect for detection is from individual SN in nearby starburst galaxies, such as M82 and NGC253 ( $D_L = 3.2$  and  $2.5$  Mpc in the Northern and Southern sky, respectively), over a negligible background, using temporal and positional coincidences with optical detections. The SN rate in these is  $\sim 0.1 \text{yr}^{-1}$  [20], much larger than in our own galaxy or in the Magellanic clouds.

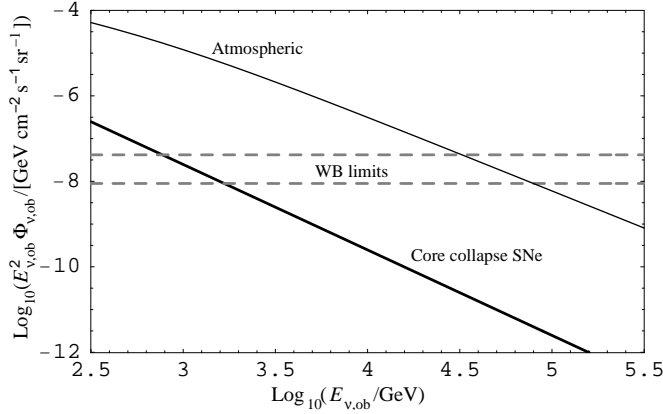


FIG. 2: Diffuse muon neutrino flux on Earth from all ( $\xi_{\text{sn}} = 1$ ,  $E_j = 10^{51.5}$  erg) core collapse SNe (heavy solid curve). The dashed curves are the cosmic ray (WB) limits, and the light full curve is the atmospheric  $\nu_\mu$  and  $\bar{\nu}_\mu$  flux. This shows that the diffuse SNe flux is unlikely to be detectable with  $\text{km}^2$  detectors. However, individual nearby SNe may be detectable, as discussed below.

To calculate the number of  $\nu_\mu$  events in a  $\text{km}^2$  detector such as IceCube, we use the fluence of Eq.(3) from each SN in the 300 GeV-300 TeV energy range, and the full detection probability depending on the source's angular position. This probability depends on the Earth's shadowing effect and the energy dependent  $\nu N$  cross section inside  $A_{\text{eff}}$  [21]. The number of  $\nu_\mu$  events from M82 and NGC253 is  $281 E_{51.5}^{3/2}$  and  $482 E_{51.5}^{3/2}$ , respectively per individual SN with its jet pointing towards us. The timing uncertainty in the optical detection of SN is  $\sim 1$  day. The corresponding atmospheric background events within  $1^\circ$  angular resolution is 0.07 for both M82 and NGC253 in the same energy range. At the quoted rate, a SN from one of these galaxies would be expected within five years. Other nearby spirals (M31, M74, M51, M101, etc, and the Virgo cluster) will also contribute. At the standard rate of 1 SNU =  $10^{-2} \text{yr}^{-1}$  per  $10^{10}$  blue solar luminosity for average galaxies, the roughly 4000 galaxies known within 20 Mpc would suggest a rate  $\gtrsim 1 \text{ SN yr}^{-1}$ . IceCube may detect roughly 1/5 of them at a level of  $\gtrsim 1.5 \nu_\mu$  events/SN.

Because of oscillations, neutrinos of all three flavors ( $\nu_\mu$ ,  $\nu_e$ ,  $\nu_\tau$ ) should reach us in equal proportion. However, only  $\nu_\mu$ 's are emitted from the sources under consideration and the total number of neutrino events (including  $\nu_e$  and  $\nu_\tau$ ) will remain the same as the  $\nu_\mu$  events we have calculated. The lack of good directional sensitivity for the  $\nu_e$  and  $\nu_\tau$  events may prevent obtaining their positional coincidence with the SN. (Also, the  $A_{\text{eff}}$  for  $\nu_e$  and  $\nu_\tau$  detection are somewhat smaller than  $\nu_\mu$ .) However the timing coincidence of  $\nu_e$  and  $\nu_\tau$  events with  $\nu_\mu$  events may still be useful to verify the neutrino oscillations at these energies, and test their common origin.

*Discussion.*— While ultra relativistic jets are thought

to be responsible for the long-duration GRB associated with a small fraction of massive core collapse SNe, mildly relativistic jets may occur in a much larger ( $\lesssim 1$ ) fraction of core collapse SNe. Such slow jets may contribute to the bounce needed for ejecting the stellar envelope, resulting in the observed SN optical display. Late time ( $\sim \text{yr}$ ) radio emission may be a signature of slow jets [11]. Such jets may also be needed to explain the apparent unusually large energies of hypernovae and the anisotropies inferred from optical polarization measurements of core collapse SNe. Here we propose, as an independent test of this model, the observation of TeV neutrinos, which may be detected in the near future with IceCube and other  $\text{km}^2$  neutrino Cherenkov detectors.

We thank T. Abel, J. Bahcall, D. Cowen, A. Gal-Yam and C. Peña-Garay for helpful discussions. We are grateful to Shin'ichiro Ando and John Beacom for pointing out some errors in the published paper. This work was supported by NSF AST0098416, the Domus Hungarica Scientiarum et Artium, the Monell Foundation, ISF and Minerva grants.

- 
- [1] K. Hirata *et al.*, Phys. Rev. Lett. **58**, 1490 (1987).
  - [2] E. Waxman and J.N. Bahcall, Phys. Rev. Lett. **78**, 2292 (1997).
  - [3] B. Zhang and P. Mészáros, Int. J. Mod. Phys. A **19**, 2385 (2004).
  - [4] P. Mészáros and E. Waxman, Phys. Rev. Lett. **87**, 171102 (2001); S. Razzaque, P. Mészáros and E. Waxman, Phys. Rev. D **68**, 083001 (2003).
  - [5] A.M. Khokhlov, *et al.*, Astrophys. J. **529**, L107 (1999).
  - [6] A.I. Macfadyen, S.E. Woosley and A. Heger, Astrophys. J. **550**, 410 (2001).
  - [7] E. Berger, *et al.*, Astrophys. J. **599**, 408 (2003).
  - [8] E. Waxman and A. Loeb, Phys. Rev. Lett. **87**, 071101 (2001).
  - [9] E. Ramirez-Ruiz, A. Celotti and M.J. Rees, Mon. Not. R. Astron. Soc. **337**, 1349 (2002).
  - [10] J. Granot and A. Loeb, Astrophys. J. **593**, L81 (2003).
  - [11] J. Granot and E. Ramirez-Ruiz, astro-ph/0403421.
  - [12] J.S. Bloom *et al.*, Astrophys. J. **506**, L105 (1998); B.M.S. Hansen, Astrophys. J. **512**, L117 (1999).
  - [13] J. Ahrens *et al.*, Astropart. Phys. **20**, 507 (2004); E. Aslanides *et al.*, astro-ph/9907432.
  - [14] S. Razzaque, P. Mészáros and E. Waxman, Phys. Rev. Lett. **90**, 241103 (2003).
  - [15] C. Porciani and P. Madau, Astrophys. J. **548**, 522 (2001).
  - [16] L. Hernquist and V. Springel, Mon. Not. R. Astron. Soc. **341**, 1253 (2003).
  - [17] P. Madau, M. della Valle and N. Panagia, Mon. Not. R. Astron. Soc. **297**, 17L (1998).
  - [18] M. Thunman *et al.*, Astropart. Phys. **5**, 309 (1996).
  - [19] J. Ahrens, *et al.*, Phys. Rev. D **66**, 012005 (2002).
  - [20] A. Alonso-Herrero *et al.*, Astron. J. **125**, 1210A (2003).
  - [21] S. Razzaque, P. Mészáros and E. Waxman, Phys. Rev. D **69**, 023001 (2004).